Geochemistry Geophysics Geosystems G3

Article
Volume 12, Number 6
15 June 2011
Q06005, doi:10.1029/2011GC003559
ISSN: 1525-2027

Published by AGU and the Geochemical Society

Tiny intraplate earthquakes triggered by nearby episodic tremor and slip in Cascadia

John E. Vidale, Alicia J. Hotovec, Abhijit Ghosh, and Kenneth C. Creager

Department of Earth and Space Sciences, University of Washington, Box 351310, Seattle, Washington 98195, USA (vidale@uw.edu)

Joan Gomberg

U.S. Geological Survey, Department of Earth and Space Sciences, University of Washington, Box 351310, Seattle, Washington 98195, USA

[1] Episodic tremor and slip (ETS) has been observed in many subduction zones, but its mechanical underpinnings as well as its potential for triggering damaging earthquakes have proven difficult to assess. Here we use a seismic array in Cascadia of unprecedented density to monitor seismicity around a moderate 16 day ETS episode. In the 4 months of data we examine, we observe five tiny earthquakes within the subducting slab during the episode and only one more in the same area, which was just before and nearby the next ETS burst. These earthquakes concentrate along the sides and updip edge of the ETS region, consistent with greater stress concentration there than near the middle and downdip edge of the tremor area. Most of the seismicity is below the megathrust, with a similar depth extent to the background intraslab seismicity. The pattern of earthquakes that we find suggests slow slip has a more continuous temporal and spatial pattern than the tremor loci, which notoriously appear in bursts, jumps, and streaks.

Components: 4400 words, 5 figures, 1 table.

Keywords: episodic tremor and slip; slow slip; triggered earthquakes.

Index Terms: 7240 Seismology: Subduction zones (1207, 1219, 1240); 7230 Seismology: Seismicity and tectonics (1207, 1217, 1240, 1242); 7203 Seismology: Body waves; 8118 Tectonophysics: Dynamics and mechanics of faulting (8004); 8104 Tectonophysics: Continental margins: convergent.

Received 10 February 2011; **Revised** 29 March 2011; **Accepted** 29 March 2011; **Published** 15 June 2011.

Vidale, J. E., A. J. Hotovec, A. Ghosh, K. C. Creager, and J. Gomberg (2011), Tiny intraplate earthquakes triggered by nearby episodic tremor and slip in Cascadia, *Geochem. Geophys. Geosyst.*, *12*, Q06005, doi:10.1029/2011GC003559.

1. Introduction

[2] Episodic tremor and slip (ETS) [*Dragert et al.*, 2001; *Obara*, 2002], which is marked by tremor, and also by observable slow slip when the episode is sufficiently long lived, displays slip with a broad spectrum of time scales [e.g., *Ghosh et al.*, 2010a, 2010b] accommodating low-stress, slow slip on many major faults [*Peng and Gomberg*, 2010]. Terminology is in flux: what we are calling ETS could be termed more generically "slow slip" by others, with ETS reserved only for larger, periodic slow slip episodes.

[3] Physical models that predict ETS's streaks, bands, slow migration, variable sensitivity to tidal stressing, and relative indifference to normal stresses are beginning to emerge. However, whether ETS influences the timing of earthquakes on the nearby locked faults, most ominously on the large asperities that will generate great earthquakes in subduction

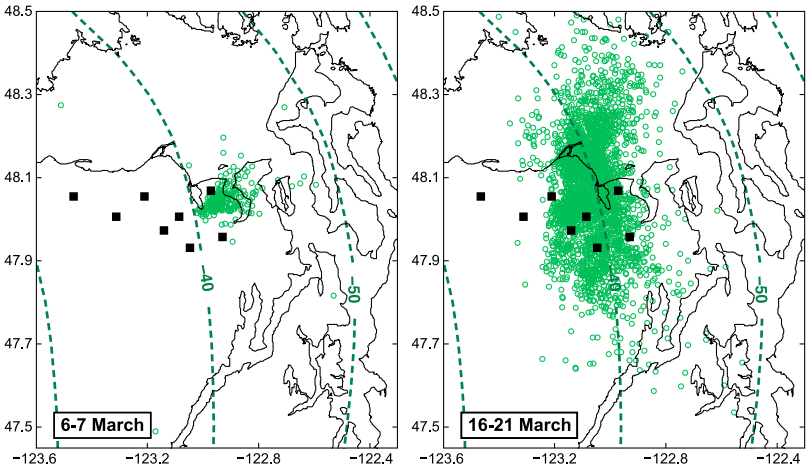

Figure 1. Map of ETS locations that occurred on (left) 6–7 March and (right) 16–21 March. Black squares mark array locations, and tiny green circles mark detections of tremor in 1 min intervals. Slab depth contours are marked with dashed lines, and numbers indicate slab depth in km.

zones near cities such as Tokyo and Seattle, remains a matter of poorly constrained speculation.

[4] Triggering of earthquakes as well as tremor has been well documented. Earthquakes trigger earthquakes, both by static stressing [e.g., *Cochran et al.*, 2004; *Stein*, 1999] and dynamic stressing from seismic waves [e.g., *Hill and Prejean*, 2007]. Studies also document that seismic waves trigger tremor [*Peng and Gomberg*, 2010; *Rubinstein et al.*, 2009]. However, up to now, there has not been a demonstration that possibly feeble ETS stresses could trigger normal fast earthquakes. The most direct link so far is that slow slip has apparently extended into seismogenic regions to cause earthquakes [*Delahaye et al.*, 2009; *Linde et al.*, 1996; *Segall et al.*, 2006]. A related observation is that slow slip can change the periodicity of nearby earthquakes on the same fault [*Kimura et al.*, 2009]. This question bears directly on the potential to forecast the likelihood of disastrous earthquakes, which often strike near regions of tremor.

[5] We closely examine the 6 to 21 March 2010 ETS episode because it occurred mostly within an area that was well instrumented by our recent EarthScope Array of Arrays dense seismometer deployment. The much larger ETS episode in August 2010, which might seem to be the more logical candidate, was too strong, too areally extensive, and too long lasting to allow such sensitive identification of the tiny earthquakes as we report here.

[6] We find five small earthquakes close in space and time to the March ETS episode. We observe only tremor without detecting slow slip, but consider that slow slip was probably present with a magnitude too small to observe, and so infer that the observed earthquakes result from the stressing of the ETS episode.

2. Data Analysis

[7] To reveal the essence of ETS, we installed the EarthScope Array of Arrays across the northeast Olympic Peninsula (Figure 1). It comprises eight ~1 km aperture arrays. Each array was populated with 10 or more three-component 4.5 Hz L-28 sensors from summer 2009 until fall 2010, and beyond. During the main ETS episode in August 2010, the instrument count was doubled with the addition of vertical component sensors, but this paper focuses on the earlier March episode filling a more limited area that the arrays covered more completely. We also detected a surplus of earthquakes compared to background rate during the main ETS episode in August, but chose to focus on the March episode for the following reasons. High-amplitude, continuous chatter from the August tremor was more overwhelming and, since tremor swept the entire region, up and downdip ETS edges were far outside the array, and the along strike edges were migrating in complicated and as yet unmapped ways. Further, since the March ETS episode already fills a larger area than the array spanned, and tremor has been observed to accumulate moment fairly linearly with time, it is not clear that much greater triggered earthquake activity directly under the array is expected for the major ETS episode.

[8] Our challenge for this project was to detect with uniform criteria as many earthquakes as possible across 4 months, from March through June 2010. In particular, we sought earthquakes close to the tremor zone where the inferred ETS stress changes would be largest. Our aim is to filter out the shallower as well as the more distant seismicity. The regional Pacific Northwest Seismic Network (PNSN) catalog contained just four earthquakes in this region during the entire first 10 months of 2010, and just one during the March ETS episode, and hence was too sparse for use. However, of the four earthquakes, one was during this 10 day episode and two others were during the 1 month major August episode hinting at an earthquake-tremor correlation.

[9] Occasional nearby earthquakes are obvious on individual seismograms, even during tremor, due to the broadband impulsive energy visible first as vertically polarized compressional waves, then a few seconds later as horizontally polarized shear waves. We enhance the P wave arrivals by filtering from 10 to 15 Hz, taking the envelope, and stacking all the vertical channels in each array. This high-frequency passband is chosen to favor earthquakes over tremor bursts. We apply the same processing to the east horizontal component with 2 to 8 Hz filtering, as S waves generally have their high frequencies attenuated, and have more power at low frequency. The east component tended to show earthquakes and tremor more strongly than the north component. This process results in 16 stacked envelopes from the 8 arrays.

[10] We produced a "detector" time series with an algorithm seeking isolated P and S arrivals with minimal coda, and with the P and S waves separated by 3 to 8 s. This S-P timing most effectively selects events about 20 to 80 km from the arrays. In detail, we compute stacked envelopes for vertical and east components of each array, and compute the ratios of peak amplitude around the time of the P (on the vertical) and S (on the east) waves to the average amplitude before and after, checking every second across the months of recording to find impulsive P and S waves with the chosen S-P differential time. We multiply the ratios computed for each array, then sum those products across all arrays. The detector relies on signal-to-noise ratio levels, and is objectively applied to all the data.

[11] Whenever the detector output exceeded a threshold, we visually examined the set of 16 envelopes to see whether an earthquake under the array had happened, and located it if it did. The number of detections per day ranged from zero for a few days to 100 during tremor. The high number during tremor arose because the algorithm was also a prolific detector of strong low-frequency earthquakes (LFEs), despite the high-pass P filtering, as strong tremor is sometimes observed up to 20 Hz, so visual discrimination was an important step.

[12] Envelope and detector snippets of three events are shown in Figure 2. Note that the high-pass filtering of the vertical components often creates mostly P energy vertical stacks. In contrast, low-pass filtering the horizontal component generally makes nearly pure S wave horizontal stacks. An LFE is distinguishable by an emergent and long time function, but unlike most tremor, has distinct P and S wave arrivals. LFEs and other pulses of tremor big enough to trigger the detector have emergent beginnings, show temporal complexity across many of the stacks, and generally occurred during intervals of strong tremor. If we have missed some earthquakes due to discarding them as tremor, our conclusions are only strengthened.

[13] We inspected times that the detector exceeded a specific threshold for the 4 months of March through June, culling 137 earthquakes in a broad neighborhood near the Array of Arrays. We stopped at the end of June because several more, smaller tremor bursts began 2 July 2010 in the same place, complicating assessment of whether later events were or were not associated with tremor.

[14] We located all events, and then rejected events that located outside the area of the map in Figure 1 and others more than 10 km above the *McCrory et al.* [2004] model interface; stress changes from ETS would likely be small and no obvious relation was seen to the timing of the tremor episode. This process revealed a total of 21 events near or below the interface within the area mapped in Figure 1, which are shown on the timeline in Figure 3, and listed in Table 1.

[15] The entire process is objective in achieving uniform sensitivity over time, except for possibly underestimating the number of events during noisy tremor. In particular, the distribution of earthquakes with distance and depth should not depend on calendar date.

[16] Locations were derived using 9 or more of the possible 16 P and S wave arrivals, with our standard PNSN XPED software, which was derived from the program Hypoinverse. For the five events during the tremor episode, and the last two at the end of June, we added picks from the surrounding Pacific Northwest Seismic Network for greater

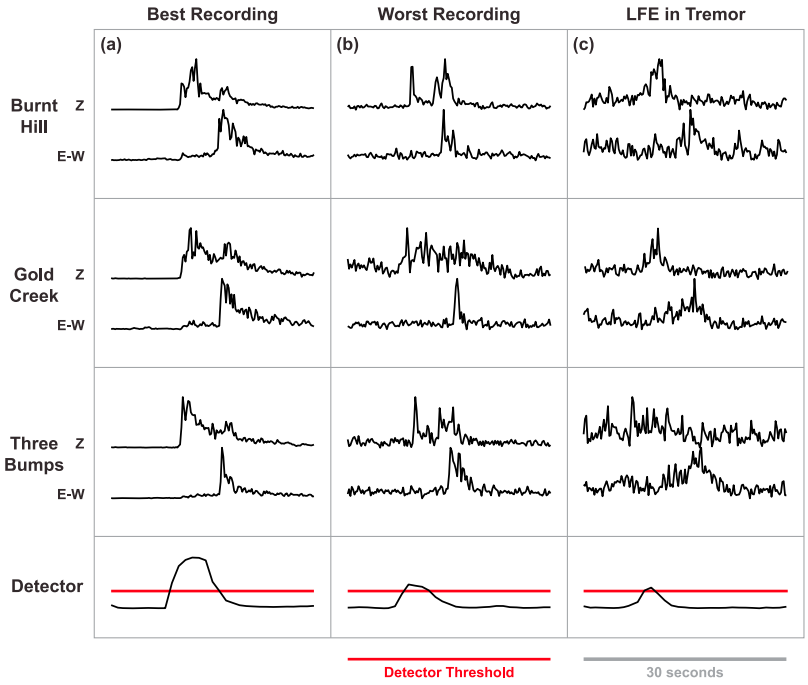

Figure 2. Comparison of the vertical and horizontal stacks from three representative arrays for (a) the largest earthquake at 12:31:13 UTC on 17 March 2010; (b) the earthquake at 12:13:20 UTC on 13 March 2010, which is the weakest of the triggered earthquakes; and (c) tremor at 13:55:50 UTC on 15 March 2010. The "Z" traces are stacks of the envelopes of 10–15 Hz band-pass-filtered vertical component seismograms across the named array. The "E–W" traces are stacks of the envelope of 2–8 Hz band-pass-filtered east–west component seismograms across the named array indicated in the *y* axis label. The detector is tuned to find isolated P waves on the vertical, followed a few seconds later by isolated S waves on the east component, detected on many arrays within a few seconds.

accuracy. The calculated depth uncertainties are 3 km or less, and listed in Table 1. We also calculated beams of the P waves from each nearby array, finding consistency of the locations with the observed slowness and angle of incidence.

[17] The amplitudes of the waves ranged downward from the largest event, measured as M1.5 by the PNSN, to amplitudes about one hundredth as large, or roughly M-0.5 (see Table 1 for estimates). These small magnitudes may explain why such triggered seismicity has not been seen before. The

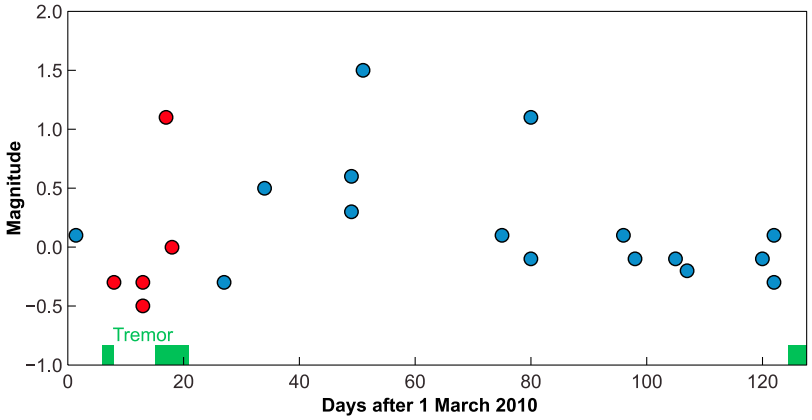

Figure 3. Timeline indicating the occurrence times of the 21 located earthquakes (circles) and tremor (green rectangles). Earthquakes during tremor are red. Magnitudes are derived simply from the amplitude of the stacks such as are shown in Figure 2 and likely have uncertainty of at least 0.3.

Table 1. Earthquakes Near Subducting Lithosphere

Month	Day	Time (UTC)	Magnitude	Latitude	Longitude	Depth (km)	Uncertainty (km)	Day
3	1	0134:42	0.1	47.62	−123.31	31.8	0.9	1
3	8	2001:22	−0.3	47.97	−123.37	46.4	0.0	8
3	13	0613:08	−0.5	48.19	−123.09	37.4	0.9	13
3	13	1136:13	−0.3	47.74	−123.19	42.1	0.9	13
3	17	1231:12	1.1[a]	48.04	−123.09	46.7	0.5	17
3	18	0408:17	0.0	47.92	−122.91	44.5	0.3	18
3	27	0229:05	−0.3	47.46	−123.13	34.4	2.0	27
4	3	2215:24	0.5	48.37	−122.89	42.9	1.5	34
4	18	1616:33	0.3	48.29	−123.33	46.0	2.1	49
4	18	2025:58	0.6	48.37	−122.91	41.8	1.7	49
4	20	1004:36	1.5[a]	47.80	−122.80	55.7	1.3	51
5	14	0119:27	0.1[a]	47.85	−123.58	35.4	1.5	75
5	19	0530:36	1.1[a]	48.33	−122.98	55.0	1.9	80
5	19	0759:56	−0.1	47.67	−123.14	38.3	1.5	80
6	4	0211:41	0.1	47.76	−122.71	49.9	1.5	96
6	6	0344:59	−0.1	48.45	−123.56	34.2	2.9	98
6	13	1103:11	−0.1	48.22	−123.13	35.0	0.9	105
6	15	0234:12	−0.2	48.26	−123.16	45.7	2.4	107
6	28	0325:42	−0.1	48.43	−123.37	34.3	3.1	120
6	30	1020:05	0.1	48.01	−123.19	46.0	0.1	122
6	30	2335:52	−0.3	47.91	−122.57	47.6	1.9	122

[a]Magnitude from PNSN catalog.

triggered earthquakes are generally smaller than the earthquakes far from the ETS patch (Figure 3). This apparent trend likely arises because as events are further from the footprint of the array, or different than the target depth range, increasing deviations from the targeted S-P times make it necessary for the events to have many arrays showing a strong signal to surpass the selection threshold.

3. Tremor Episode and Earthquakes

[18] The patch of the subduction interface on which this episode appeared has been observed to repeatedly host ETS. In the previous 5 years, this patch slipped in 4 major ETS episodes and at least 11 smaller episodes. The iterations varied in spatial extent, duration, and recurrence interval, with March 2010 being a middling episode.

[19] The spatial distribution of tremor and earthquakes is shown in Figure 4. Tremor has been observed in Cascadia [*Wech*, 2010] and Japan [*Obara*, 2010] to start downdip and propagate up with time. Tremor locations shown in this study are derived with a multibeam backprojection technique that applies beam-forming at each array and backprojects the best slownesses to locate tremor sources [*Ghosh et al.*, 2011]. Figure 1 shows that this episode follows the same pattern, with a deep burst of tremor activity on 6 and 7 March, then more prolonged and shallowing activity starting late on 13 March. The tremor locations are only constrained horizontally. We do not have useful depth resolution yet, possibly due to unmodeled velocity structure in this region.

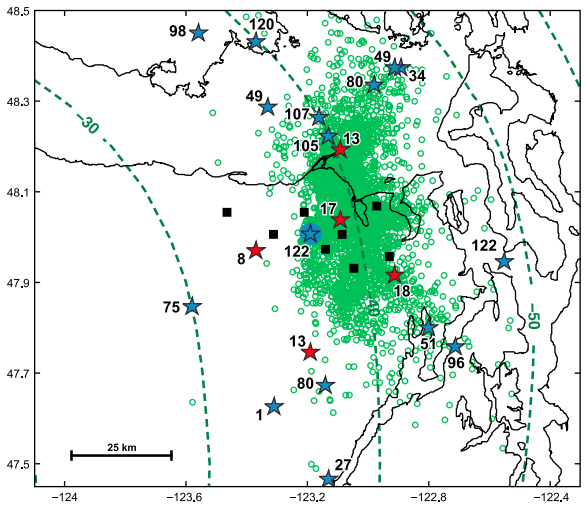

Figure 4. Map of ETS and earthquake locations. Tiny green circles mark detections of tremor in 1 min intervals, red stars indicate earthquakes during the tremor episode, and blue stars are earthquakes at other times. The blue circle marks the earthquake striking 2 days before and nearby the tremor in July. Numbering indicates how many days after 1 March the earthquakes occurred. Black squares mark array locations, slab depth contours are marked with dashed lines, and numbers indicate slab depth in km.

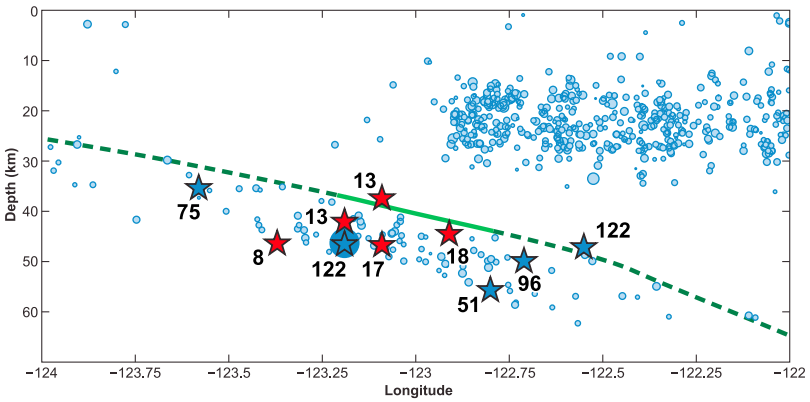

Figure 5. Cross section of earthquakes between latitudes 47.75°N and 48.25°N (stars colored the same as in Figure 4), background earthquakes (blue circles), slab interface (green line) [*McCrory et al.*, 2004], and tremor extent (solid portion of green line). Circled blue star is the same earthquake highlighted in Figure 4. The background seismicity is taken from the years 2000 to 2010 and located by the PNSN using the same velocity structure as we used to locate the events with the Array of Arrays. There was also considerable seismicity detected in the crust in this experiment, but its timing was unrelated to the tremor episode, and so it is omitted from Figure 5 and Table 1 for simplicity.

[20] The map and cross section of seismicity in Figures 4 and 5 shows the structural setting of the tremor and earthquakes. The earthquakes locate near the updip limit of the patch of strong tremor, distributed in depth consistent with the range observed for background seismicity located by the PNSN. Simultaneous tomography and relocation for this region [*Preston et al.*, 2003] indicates background seismicity fills the subducting crust and may extend down into the subducting mantle.

[21] The timing of earthquakes near the tremor, combined with their locations, indicates that the tremor and earthquakes are related. Five of the six earthquakes that strike in the area near the tremor are either in the gap between 7 March and late on 13 March, or during the prolonged burst of tremor between 13 and 21 March. The only other event that strikes within the same area was just 2 days prior to and only 10 km from the next minor tremor episode, which started 2 July, and so likely also reflects proximity to slow slip, which again appears to have started before tremor appeared.

[22] The rate of earthquakes across the entire area shown in Figure 4 is several times higher when it is 2 or fewer days from tremor activity than the rest of the time, with 7 earthquakes in 15 days versus 14 earthquakes in 107 days. Statistics are inappropriate to apply to such comparisons centered on a half dozen hits drawn after looking at the pattern of activity.

[23] While dense instrumentation and novel analysis were necessary to find these small events, similar instrumentation is becoming less rare, and the results in this paper should be able to be quickly checked and extended.

4. Interpretation of Earthquakes and ETS

[24] We infer that slow slip is likely occurring at, and tremor emanating from, the plate interface at the solid green line in Figure 5 [*Brown et al.*, 2009]. Most of the earthquakes triggered from the stresses of the inferred slow slip are located below the model plate interface, within the subducting crust and perhaps mantle. This relative location of tremor and earthquakes is similar to the spatial geometry observed in Japan [*Shelly et al.*, 2006], although the temporal correlation we report on herein has not been documented elsewhere.

[25] The timing of the six potentially triggered earthquakes suggests slow slip is more continuous than tremor in the ETS. The event on 8 March strikes more than a day after the initial tremor has ceased to be observable, although similar to aftershocks, the delay might result from reequilibration to the stress changes induced by the tremor. Harder to dismiss are the two earthquakes on 13 March, which are some distance from the initial burst of tremor and come 20 and 12 h before the tremor resumes. The two events on 13 March occur on either edge of the eventual tremor zone, suggesting that much of the zone is already undergoing slow slip. The updip event on 30 June, 2 days before the

resumption of tremor, also suggests slow slip can precede tremor.

[26] The earthquakes concentrate near the updip limit of tremor, suggesting the stress concentration is greatest there, and is consistent with observations [*Obara*, 2010; *Wech*, 2010] of tremor generally starting deep and migrating updip. Farther updip corresponds with more episodic tremor bursts rather than continual tremor, which likely indicates the ability to build up more stress updip. Alternatively, the slow slip event engenders slab pull on the updip region, which would encourage normal faulting, which is the dominant focal mechanism of intraslab activity [*Green and Houston*, 1995]. A third factor is that slow slip tends to concentrate at shallower depths than tremor for ETS episodes, so perhaps the earthquakes are really centered around the slow slip [*Peng and Gomberg*, 2010].

[27] The coincidence of ETS and these six earthquakes shows intraplate slab earthquakes are at least sometimes triggered by nearby episodic slow slip. ETS events have been shown to have a magnitude-frequency distribution similar to earthquakes, with many small ETS events for each large event, so there might be many slow episodes near the plate interface. The presence of accelerated strain from nearby slow slip events might help explain the presence of intraslab earthquakes at depths and temperatures that challenge current rheological understanding [*Green and Houston*, 1995], although we have no detailed model in mind.

[28] There are also two distinct zones of tremor in Figure 4: a 30 km core with a high density of tremor occurrence, and a more diffuse region about twice as large and centered more to the south and east with a lower density of tremor. Even the larger zone is mostly free of earthquakes for the 4 month period, very speculatively suggesting it is not as prone to slow slip episodes as the core, and rather the interface can only maintain lower stress in the outer halo.

[29] A question of great practical interest is the power of ETS to trigger damaging earthquakes, either deeper in the subduction zone, such as in the 2001 Nisqually earthquake [*Kao et al.*, 2008] and the 2009 Padang earthquake [*McCloskey et al.*, 2010], or shallower on the locked megathrust [*Segall and Bradley*, 2010]. The observation of these triggered small earthquakes is a start, but extrapolating to the nucleation sites of damaging earthquakes, and from these nanoquakes to magnitude 7 to 9 earthquakes will require further work. However, it is now clear that ETS most likely triggers normal earthquakes in a measurable way.

Acknowledgments

[30] Discussions with Heidi Houston and Herb Dragert and a thorough review from Debi Kilb helped improve the manuscript. The entire Array of Arrays team did extensive fieldwork to acquire these data, which were essential for this work.

References

Brown, J. R., G. C. Beroza, S. Ide, K. Ohta, D. R. Shelly, S. Y. Schwartz, W. Rabbel, M. Thorwart, and H. Kao (2009), Deep low-frequency earthquakes in tremor localize to the plate interface in multiple subduction zones, *Geophys. Res. Lett.*, *36*, L19306, doi:10.1029/2009GL040027.

Cochran, E. S., J. E. Vidale, and S. Tanaka (2004), Earth tides can trigger shallow thrust fault earthquakes, *Science*, *306*(5699), 1164–1166, doi:10.1126/science.1103961.

Delahaye, E. J., J. Townend, M. E. Reyners, and G. Rogers (2009), Microseismicity but no tremor accompanying slow slip in the Hikurangi subduction zone, New Zealand, *Earth Planet. Sci.Lett.*, *277*(1–2), 21–28, doi:10.1016/j.epsl.2008.09.038.

Dragert, H., K. L. Wang, and T. S. James (2001), A silent slip event on the deeper Cascadia subduction interface, *Science*, *292*, 1525–1528, doi:10.1126/science.1060152.

Ghosh, A., J. E. Vidale, J. R. Sweet, K. C. Creager, A. G. Wech, and H. Houston (2010a), Tremor bands sweep Cascadia, *Geophys. Res. Lett.*, *37*, L08301, doi:10.1029/2009GL042301.

Ghosh, A., J. E. Vidale, J. R. Sweet, K. C. Creager, A. G. Wech, H. Houston, and E. E. Brodsky (2010b), Rapid, continuous streaking of tremor in Cascadia, *Geochem. Geophys. Geosyst.*, *11*, Q12010, doi:10.1029/2010GC003305.

Ghosh, A., J. E. Vidale, and K. C. Creager (2011), Tremor depth using array of arrays in Cascadia, paper presented at SSA Annual Meeting, Seismol. Soc. of Am., Memphis, Tenn.

Green, H. W., and H. Houston (1995), The mechanics of deep earthquakes, *Annu. Rev. Earth Planet. Sci.*, *23*, 169–213, doi:10.1146/annurev.ea.23.050195.001125.

Hill, D. P., and S. Prejean (2007), Dynamic triggering, in *Treatise on Geophysics*, vol. 4, *Earthquake Seismology*, edited by H. Kanamori, pp. 257–291, Elsevier, Boston, Mass.

Kao, H., K. Wang, R. Y. Chen, I. Wada, J. H. He, and S. D. Malone (2008), Identifying the rupture plane of the 2001 Nisqually, Washington, earthquake, *Bull. Seismol. Soc. Am.*, *98*(3), 1546–1558, doi:10.1785/0120070160.

Kimura, H., K. Kasahara, and T. Takeda (2009), Subduction process of the Philippine Sea Plate off the Kanto district, central Japan, as revealed by plate structure and repeating earthquakes, *Tectonophysics*, *472*(1–4), 18–27, doi:10.1016/j.tecto.2008.05.012.

Linde, A. T., M. T. Gladwin, M. J. S. Johnston, R. L. Gwyther, and R. G. Bilham (1996), A slow earthquake sequence on the San Andreas fault, *Nature*, *383*, 65–68.

McCloskey, J., D. Lange, F. Tilmann, S. S. Nalbant, A. F. Bell, D. H. Natawidjaja, and A. Rietbrock (2010), The September 2009 Padang earthquake, *Nat. Geosci.*, *3*(2), 70–71, doi:10.1038/ngeo753.

McCrory, P. A., J. L. Blair, D. H. Oppenheimer, and S. R. Walter (2004), Depth to the Juan de Fuca slab beneath the Cascadia subduction margin: A 3-D model for sorting earthquakes, *U.S. Geol. Surv. Data Ser.*, *91*.

Obara, K. (2002), Nonvolcanic deep tremor associated with subduction in southwest Japan, *Science*, *296*(5573), 1679–1681, doi:10.1126/science.1070378.

Obara, K. (2010), Phenomenology of deep slow earthquake family in southwest Japan: Spatiotemporal characteristics and segmentation, *J. Geophys. Res.*, *115*, B00A25, doi:10.1029/2008JB006048.

Peng, Z. G., and J. Gomberg (2010), An integrated perspective of the continuum between earthquakes and slow-slip phenomena, *Nat. Geosci.*, *3*(9), 599–607, doi:10.1038/ngeo940.

Preston, L. A., K. C. Creager, R. S. Crosson, T. M. Brocher, and A. M. Trehu (2003), Intraslab earthquakes: Dehydration of the Cascadia slab, *Science*, *302*, 1197–1200, doi:10.1126/science.1090751.

Rubinstein, J. L., J. Gomberg, J. E. Vidale, A. G. Wech, H. Kao, K. C. Creager, and G. Rogers (2009), Seismic wave triggering of nonvolcanic tremor, episodic tremor and slip, and earthquakes on Vancouver Island, *J. Geophys. Res.*, *114*, B00A01, doi:10.1029/2008JB005875.

Segall, P., and A. M. Bradley (2010), Numerical simulation of slow slip and dynamic rupture in the Cascadia Subduction Zone, Abstract S13D-05 presented at 2010 Fall Meeting, AGU, San Francisco, Calif.

Segall, P., E. K. Desmarais, D. Shelly, A. Miklius, and P. Cervelli (2006), Earthquakes triggered by silent slip events on Kilauea volcano, Hawaii, *Nature*, *442*, 71–74, doi:10.1038/nature04938.

Shelly, D. R., G. C. Beroza, S. Ide, and S. Nakamula (2006), Low-frequency earthquakes in Shikoku, Japan, and their relationship to episodic tremor and slip, *Nature*, *442*(7099), 188–191, doi:10.1038/nature04931.

Stein, R. S. (1999), The role of stress transfer in earthquake occurrence, *Nature*, *402*, 605–609, doi:10.1038/45144.

Wech, A. (2010), Tremor, Ph.D. thesis, Univ. of Wash., Seattle.